0022-3565/08/3273-991–1000$20.00
THE JOURNAL OF PHARMACOLOGY AND EXPERIMENTAL THERAPEUTICS
JPET 327:991–1000, 2008

Vol. 327, No. 3
142307/3410404
Printed in U.S.A.

Kinetic and Thermodynamic Assessment of Binding of Serotonin Transporter Inhibitors

Renee S. Martin, Robert A. Henningsen, Alexander Suen, Subbu Apparsundaram, Becky Leung, Zhongjiang Jia, Rama K. Kondru, and Marcos E. Milla

Departments of Biochemical Pharmacology (R.S.M., R.A.H., A.S., S.A., B.L., M.E.M.), Pharmaceutics (Z.J.), and Medicinal Chemistry (R.K.K.), Roche Pharmaceuticals, Palo Alto, California

Received June 13, 2008; accepted September 16, 2008

ABSTRACT

Several serotonin reuptake inhibitors are in clinical use for treatment of depression and anxiety disorders. However, to date, reported pharmacological differentiation of these ligands has focused mainly on their equilibrium binding affinities for the serotonin transporter. This study takes a new look at antidepressant binding modes using radioligand binding assays with [^{3}H]*S*-citalopram to determine equilibrium and kinetic rate constants across multiple temperatures. The observed dissociation rate constants at 26°C fall into a narrow range for all molecules. Conversely, association rate constants generally decreased with increasing equilibrium binding affinities. Consistent with this, the measured activation energy for *S*-citalopram association was relatively large (19.5 kcal · mol^{-1}), suggesting conformational change upon ligand binding. For most of the drugs, including citalopram, the enthalpy (ΔH^O) and entropy ($-T\Delta S^O$) contributions to reaction energetics were determined by van't Hoff analyses to be roughly equivalent (25–75% ΔG^O) and to correlate (positively for enthalpy) with the polar surface area of the drug. However, the binding of the drug fluvoxamine was predominantly entropically driven. When these data are considered in the context of the physicochemical properties of these ligands, two distinct binding modes can be proposed. The citalopram-type binding mode probably uses a polar binding pocket that allows charged or polar interactions between ligand and receptor with comparatively small loss in enthalpy due to dehydration. The fluvoxamine-type binding mode is fueled by energy released upon burying hydrophobic ligand moieties into a binding pocket that is flexible enough to suffer minimal loss in entropy from conformational constraint.

Inhibitors of the serotonin transporter (SERT) have long been in clinical use for treatment of depression and anxiety, predating even the molecular identification of the target (Blakely et al., 1991). As such, SERT is the target of a large number of clinically proven drugs from diverse chemotypes (Fig. 1) that act by blocking transit of 5-hydroytryptamine (serotonin) (5-HT) through the transporter. Many reports describe the equilibrium binding properties of members of this class of drugs with SERT as well as potency for inhibition of 5-HT reuptake (Blakely et al., 1994; Tatsumi et al., 1997; Nemeroff and Owens, 2003; Rothman and Baumann, 2003). Although the three-dimensional structure of SERT has not yet been elucidated, crystal structures have been determined for other members of the 12 transmembrane domain major facilitator superfamily. Of these, the most homologous transporter to SERT is the bacterial leucine transporter LeuT (Yamashita et al., 2005). A three-dimensional model of SERT based on the published crystal structure of LeuT places several key amino acid residues that interact with SERT inhibitors along the proposed substrate permeation path (Ravna et al., 2006a).

Recently, crystal structures of LeuT in complex with high-affinity SERT inhibitors were reported (Singh et al., 2007; Zhou et al., 2007). These structures identify the substrate (leucine) and inhibitor binding sites as nonoverlapping. Furthermore, the importance of specific mutations at I172M and Y95F on inhibitor potency but not 5-HT transport interaction suggests that the substrate-inhibitor binding interactions may be nonoverlapping in SERT as well (Henry et al., 2006). However, very recent data (Apparsundaram et al., 2008) demonstrate that 5-HT and the SERT inhibitors bind in a mutually exclusive, competitive manner at SERT.

Data describing the kinetics of ligand association and dissociation remain sparse for this transporter. Recent reports have identified a new binding site that, based on its influence over the dissociation kinetics of [^{3}H]*S*-citalopram, allosteri-

This study was wholly funded by Roche Pharmaceuticals, Palo Alto, CA.
Article, publication date, and citation information can be found at http://jpet.aspetjournals.org.
doi:10.1124/jpet.108.142307.

ABBREVIATIONS: SERT, serotonin transporter; 5-HT, 5-hydroxytryptamine (serotonin); LeuT, leucine transporter; HEK, human embryonic kidney; h, human; PSA, polar surface area.

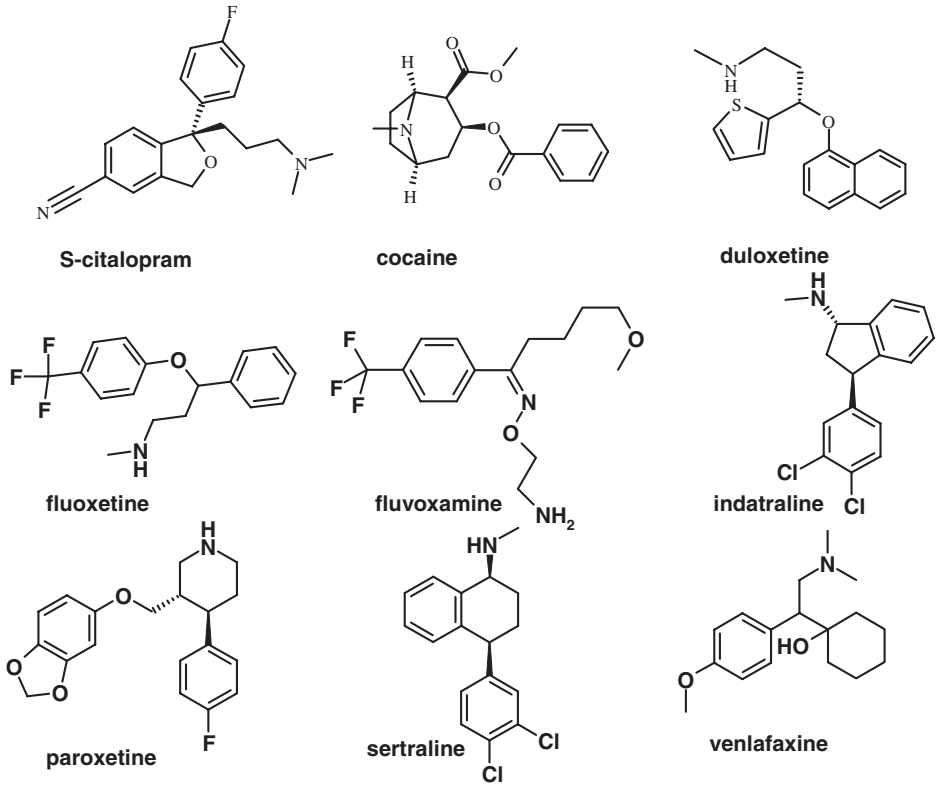

Fig. 1. Chemical structures of SERT inhibitors used in this study.

cally modulates binding of *S*-citalopram and other high-affinity inhibitors (Chen et al., 2005a,b).

To date, only a limited number of studies have undertaken thermodynamic assessment of membrane-bound receptor targets. In particular, the entropic nature of substrate interaction with the dopamine transporter differed from the enthalpic binding interactions of inhibitors (Bonnet et al., 1990). Other studies with G protein-coupled receptors or ion channels suggest that the interplay of enthalpy or entropy components may provide a way of differentiating agonist from antagonist interactions with the target receptor (Borea et al., 2000).

In this report, we used a radioligand binding approach to determine the effects of temperature on equilibrium and kinetic rate constants for a set of clinically relevant SERT inhibitors. Our goal was to reveal the energetic components driving their interactions with this transporter and to determine whether conformational rearrangement within SERT or ligand conformational flexibility plays a role in the binding reaction. We analyze our results in the context of previous studies that focused on other systems, and we highlight the potential for pharmacological differentiation in drug development.

Materials and Methods

Radioligand binding experiments were conducted in membranes derived from HEK293 cells stably expressing recombinant human SERT (acquired from Randy Blakely, Vanderbilt University, Nashville, TN) (Blakely et al., 1994). Cells were cultured in Dulbecco's modified Eagle's medium supplemented with 10% fetal bovine serum and harvested for membrane preparation by homogenization in buffer (ice-cold 50 mM Tris, pH 7.4, with 1× Complete protease inhibitor cocktail; Roche Molecular Systems, Inc., Alameda, CA). The structures of all ligands used in this study have been published previously (Claassen et al., 1977; Wong et al., 1993; Partilla et al., 2000; White et al., 2005; Ravna et al., 2006b) and are presented in Fig. 1. Enantiomerically pure tritium-labeled *S*-citalopram (84.8 Ci/mmol) was synthesized by Mohammad Masjedizadeh and colleagues in the Department of Radiochemistry at Roche (Palo Alto, CA); purity was confirmed by high-performance liquid chromatography to be >97%.

Equilibrium Binding. The ligand affinities at human SERT were determined using hSERT-HEK membranes under equilibrium binding conditions in assay buffer composed of 126 mM NaCl, 2.7 mM KCl, 10 mM Na_2HPO_4, and 1.76 mM KH_2PO_4, pH 7.4. [^{3}H]*S*-citalopram (0.3–100 nM) was incubated with hSERT-HEK membranes (10–20 $\mu g \cdot ml^{-1}$) in the absence or presence of 10 μM paroxetine (to define nonspecific binding) for 2 to 5 h to determine its dissociation affinity constant $K_D = (k_{-1})/(k_{+1})$ as well as the receptor expression level (B_{max}) of the membranes. For unlabeled molecules, the equilibrium dissociation affinity constants (K_I) were determined by coincubating unlabeled molecule (serially diluted over a million-fold concentration range) with [^{3}H]*S*-citalopram (1–5 nM) and hSERT-HEK membranes. As negative and positive controls, membranes in separate experimental wells were incubated with [^{3}H]*S*-citalopram and a volume of assay buffer or paroxetine (10 μM) to define total and nonspecific binding, respectively. In all cases, incubation was ended by filtration with ice-cold 50 mM Tris, pH 7.4, on GF/B filters (PerkinElmer Life and Analytical Sciences, Boston, MA). Filters were soaked in MicroScint-20 scintillation cocktail (PerkinElmer Life and Analytical Sciences) for at least 3 h before quantification of filter-trapped radioactivity using a PerkinElmer TopCount plate reader. Competition binding data were analyzed by nonlinear regression to a four-parameter hyperbolic function to estimate all of maximal, minimal, Hill slope, and IC_{50} values; K_I estimates were calculated from observed IC_{50} values using the Cheng-Prusoff equation (Cheng and Prusoff, 1973). Affinities are presented as the mean and standard deviations determined over two to four repeat determinations.

Kinetic Analysis of Ligand Binding. Association and dissociation rate constants for [^{3}H]*S*-citalopram or at hSERT-HEK membranes were determined by time-controlled exposure of radioligand

to membrane using the assay buffer and conditions described above. In dissociation, radioligand was allowed to pre-equilibrate with membrane for 2 to 5 h before initiation of dissociation by 100-fold dilution of the reaction mixture using assay buffer. The progress of ligand dissociation was followed in separate assay wells in which reaction was stopped at fixed time points by filtration using ice-cold 50 mM Tris, pH 7.4, on GF/B filters. Data were analyzed by nonlinear regression using exponential growth or decay curves to determine the observed exponential growth constant (k_{obs}), the dissociation rate constant (k_{-1}), and half-life ($t_{1/2}$). Additional linear regression analyses allowed inference of k_{+1} and k_{-1} from estimates of k_{obs} at different radioligand concentrations using the following relationship: $k_{obs} = k_{+1} \times [\text{radioligand}] + k_{-1}$. Data are presented as the mean rate constant determined over two to four repeat determinations. In a limited number of experiments, the dissociation rate of [^{3}H]paroxetine (Amersham Life Technologies, Chalfont, St Giles, UK) was determined using similar methods.

Dissociation rate constants for nonradiolabeled ligands were determined using a "competitive dissociation" method where test ligand was preincubated (at three times its equilibrium affinity, K_I, with an aim to occupy 75% of the binding sites to increase signal size) with hSERT-HEK membranes for 2 to 5 h at room temperature followed by addition of [^{3}H]*S*-citalopram at a concentration 20 to 30 times greater than its K_D value. This high concentration of radioligand was selected such that the bound radioactivity observed in the absence of competing unlabeled ligand at the shortest time point was less than 20% of the maximal (equilibrium) binding level. In this way, the impact of radioligand association rate was minimized, and rate of unlabeled ligand dissociation was directly inferred from the observed rate of radioligand binding using nonlinear regression to a simple exponential decay function as mentioned above. As with the methods described above for measuring radioligand dissociation, reaction was terminated at controlled time points by filtration with ice-cold 50 mM Tris, pH 7.4, on GF/B filters.

Analysis of Reaction Thermodynamics. Additional analysis of the equilibrium or kinetic binding constants, determined across various temperatures, were conducted to determine thermodynamic parameters for Gibbs free energy, enthalpy, entropy, and activation energy (E_a) using van't Hoff and Arrhenius plots. These thermodynamic relationships are described by the equations below:

$$\text{Gibbs free energy} = \Delta G^O = \Delta H^O - T\Delta S^O = RT\ln K_A \quad (1)$$

$$\ln(k_{+1}) = \ln A - \frac{E_a}{RT} \quad (2)$$

where R is the gas constant (1.985 calories per degree Kelvin); T is the temperature in Kelvin; ΔH and ΔS are the changes in enthalpy and entropy of the system, respectively; K_A is the association binding constant of the ligand at the receptor (i.e., $1/K_D$), k_{+1} is the association rate constant for the reaction; A is the Arrhenius constant; and E_a the excitation energy for the reaction in question.

Measurement of Physicochemical Properties. The pK_a and log P values were determined in 0.15 M KCl aqueous solution at 25.0 ± 0.5°C using a Sirius GLpKa titrator (Sirius Analytical Instrument Ltd., East Sussex, UK). For pK_a measurement, triplicate runs were performed in each sample vial. Two to 4 mg of drug was dissolved in 15 ml of 0.15 M KCl. The titration assays were performed from pH 3 to 11 under argon atmosphere using standardized 0.5 M HCl and 0.5 M KOH as titrants. A difference curve of average number of bound protons versus pH was derived by subtracting the blank titration curve (titration in 20 ml of 0.15 M KCl aqueous solution only) from the sample titration curve. The aqueous pK_a values were obtained by nonlinear regression using pKaLOGP software version 5.2a (Sirius Analytical Instrument Ltd.). For log P measurement, the general titration procedure and data analysis were performed as described above. Titrations were performed in the water/*n*-octanol phases at three different volume ratios in each sample vial. In the presence of *n*-octanol, the compound partitions between the aqueous phase and the *n*-octanol phases as prescribed by the number of neutral and charged species. The log P values were calculated from the differences in pK_a values observed in *n*-octanol and aqueous phases across the different *n*-octanol/water volume ratios tested. The log $D^{7.4}$ (at pH 7.4) was calculated from log P and pK_a values using the following equation for monobases, $\log D = \{\log[10^{(\text{pH} + \log P - pK_a)})/(1 + 10^{(\text{pH} - pK_a)}]\}$, where pH = 7.4.

Conformational Analysis of the Ligands. The conformations for the small-molecule ligands are generated using OMEGA program (OpenEye Scientific Software, Santa Fe, NM) (Boström et al., 2003; Perola and Charifson, 2004). The maximal number of output conformers was set to 200, and all conformers with an energy difference to the global minimum of >10.0 kcal · mol^{-1} are rejected.

Results

Equilibrium Binding. Binding of [^{3}H]*S*-citalopram to SERT under equilibrium conditions was fully saturable over the nanomolar range (Fig. 2A). Dissociation constants (K_D or K_I) for [^{3}H]*S*-citalopram and unlabeled test molecules at room temperature (Table 1) were similar to those reported previously (Blakely et al., 1994; Tatsumi et al., 1997; Nemeroff and Owens, 2003; Rothman and Baumann, 2003; Chen et al., 2005a). Scatchard transformation of the saturation binding data for [^{3}H]*S*-citalopram resulted in a straight line with a unity Hill slope, indicating a simple 1:1 interaction between ligand and transporter that saturated over the concentration range tested (Fig. 2B). Likewise, Hill slopes observed for the unlabeled inhibitors in the study were not

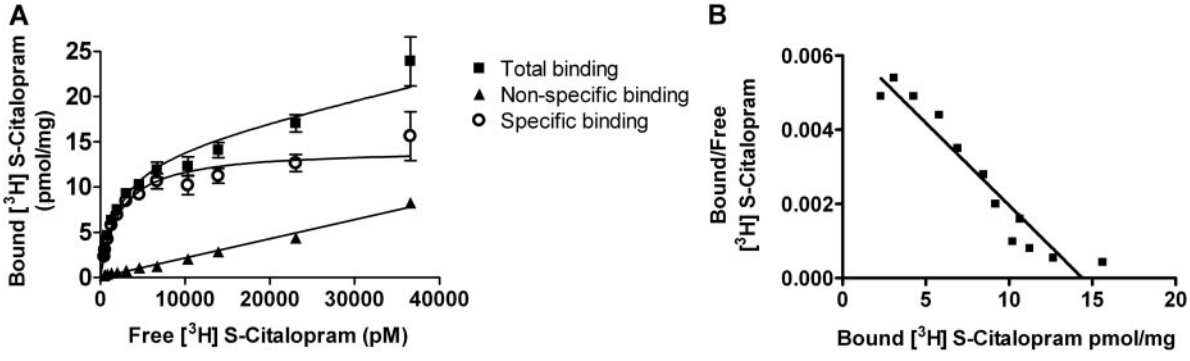

Fig. 2. Saturation binding isotherm (A) and Scatchard transformation (B) of [^{3}H]*S*-citalopram at hSERT-HEK cell membranes. Nonspecific binding is determined in the presence of 10 μM paroxetine. Data are presented for a representative experiment and show means and standard deviations of triplicate determinations for each test condition.

TABLE 1

Equilibrium binding affinities and kinetic rate constants for [^{3}H]*S*-citalopram and various transporter inhibitors at hSERT-HEK membranes

Values represent mean ± S.D. determined at room temperature from two to six independent replicate experiments (for which representative data is shown in Fig. 6). Association rate constants were calculated from observed dissociation rate constants and equilibrium affinities from the equation $k_{+1} = (k_{-1}/K_D)$ in all cases except [^{3}H]*S*-citalopram for which the constant was experimentally determined (as shown in Fig. 5).

Ligand	Equilibrium Affinity pK_D or pK_I	Equilibrium Affinity K_D or K_I	Observed Dissociation Rate Constant, k_{-1}	Observed Dissociation Half-Life, $t_{1/2}$	Calculated (or Observed) Association Rate Constant $k_{+1} \times 10^6$
	−log M	*nM*	s^{-1}	*s*	$M^{-1} \cdot s^{-1}$
[^{3}H]*S*-citalopram	8.68 ± 0.13	2.09	0.001 ± 0.0001	666 ± 48	0.48 + 0.06
S-Sitalopram	8.87 ± 0.19	1.35	0.002 ± 0.004	645 ± 111	1.48 + 0.14
Cocaine	6.40 ± 0.18	398.1	>0.01	<70	>0.02
Duloxetine	9.75 ± 0.14	0.18	0.002 ± 0.0014	384 ± 156	11.25 + 4.1
Fluoxetine	8.48 ± 0.24	3.31	0.003 ± 0.0004	221 ± 27	0.91 + 0.12
Fluvoxamine	8.17 ± 0.09	6.76	0.006 ± 0.0036	150 ± 12	0.89 + 0.06
Indatraline	8.71 ± 0.12	1.95	0.002 ± 0.0003	449 ± 74	1.03 + 0.13
Paroxetine	9.93 ± 0.43	0.12	0.001 ± 0.0009	1335 ± 868	8.51 + 7.36
Sertraline	9.07 ± 0.19	0.85	0.001 ± 0.0002	497 ± 67	1.17 + 0.23
Venlafaxine	7.79 ± 0.10	16.22	0.004 ± 0.005	458 ± 95	0.25 + 0.02

significantly different from unity (data not shown). The Gibbs free energy of dissociation, calculated from the equilibrium dissociation constants, fell within the range of −10.6 to −12.7 kcal · mol^{-1} (Table 2).

The affinity of SERT varied with temperature for both [^{3}H]*S*-citalopram and the unlabeled SERT inhibitors, with K_D values increasing with temperature in most cases. The van't Hoff analysis revealed a linear relationship between the natural logarithm of the equilibrium association constant ($\ln K_A = -\ln K_D$) and 1/T over the temperature range tested for [^{3}H]*S*-citalopram as well as for all of the unlabeled SERT inhibitors tested (Figs. 3A and 4). For every ligand assayed, estimates of enthalpy and entropy (ΔH^O and ΔS^O, respectively) were derived from the slope and y-intercept of van't Hoff plots (Fig. 4; Table 2). For [^{3}H]*S*-citalopram, these estimates were not different from those observed with unlabeled *S*-citalopram based on 95% confidence intervals (Table 2). The relative contributions of entropic ($-T\Delta S^O$) and enthalpic (ΔH^O) changes to the binding energetics were roughly equivalent for all drugs (each contributing 25–75% ΔG^O) except for fluvoxamine, which was entropy-driven. The measured entropic and enthalpic contributions were found to be inversely correlated with each other ($P < 0.0001$; Fig. 11A).

In all cases, the relationships between $\ln K_A$ and 1/T, identified from the van't Hoff plots, were linear. Furthermore, the equilibrium binding affinities and Gibbs free energies increased linearly with temperature (exemplified by [^{3}H]*S*-citalopram in Fig. 3B), suggesting a temperature dependence of ΔH. Under the assumption that entropy was temperature-independent, the enthalpy at every temperature was calculated from $\Delta H = -RT(\ln K_A) + T\Delta S$ and was found to vary linearly with temperature. The heat capacities (C_p) of the binding reactions were estimated from the slopes of ΔH versus T to fall in the narrow range of 0.01 to 0.03 kcal · mol^{-1} · K^{-1} for all ligands tested and generally followed a rank order similar to that of the pK_D values (−log M).

Kinetic Analysis of Ligand Binding. The association and dissociation rate constants (k_{+1} and k_{-1}, respectively) for [^{3}H]*S*-citalopram binding were 0.5×10^6 M$^{-1} \cdot$ s^{-1} and 0.001 s^{-1}, respectively (Fig. 5). [^{3}H]*S*-citalopram association to the transporter was fast at 32 nM, reaching maximal binding levels in less than 120 s (Fig. 5). This rapid association was exploited to determine indirectly the dissociation rate constants for all of the SERT inhibitors tested except cocaine, for which the observed dissociation rate was faster than could be measured under these experimental conditions. As a validation of these techniques, the observed dissociation rate constant of unlabeled *S*-citalopram using competitive dissociation methods was similar to that for [^{3}H]*S*-citalopram determined by assay dilution (0.001–0.002 s^{-1}, corresponding to a half-life of 645–666 s; Figs. 5C and 6A). Likewise, the dissociation half-lives of [^{3}H]paroxetine and unlabeled paroxetine, determined by dilution and competitive dissociation, respectively, fall within observed experimental variability (1335 ± 868 and 2843 ± 1000 s). For all of the other SERT inhibitors, the dissociation rate constants fell within a very narrow range (0.001–0.006 s^{-1}, corresponding to half-lives of 149-1335 s; Fig. 6) at 25°C, with a nonsignificant tendency

TABLE 2

Calculated Gibbs free energy (ΔG^O) and estimated enthalpic and entropic contributions to antidepressant drug binding to hSERT

Enthalpic and entropic contributions to antidepressant drug binding were calculated from the observed changes in equilibrium association constants (K_A) with temperature (4–42°C). Specifically, estimates of enthalpy (ΔH^O) and entropy (ΔS^O) associated with binding at SERT were made using the slope and y-intercept, respectively, as described in the van't Hoff equation, $\ln(K_A) = -(\Delta H/R)(1/T) + (\Delta S/R)$, where K_A is the inverse of the equilibrium dissociation constant K_I or K_D. Changes in Gibbs free energy (ΔG^O) were calculated for each drug using the equation $\Delta G^O = -RT\ln(K_A)$ at room temperature (24–26°C).

	Slope	y-Intercept	ΔS^O	ΔH^O	$-T\Delta S^O$ at 24°C (or 26°C)	ΔG^O kcal · mol^{-1} from $RT\ln K_D$
			Kcal · mol^{-1} · K^{-1}	*Kcal · mol^{-1}*		
[^{3}H]*S*-Citalopram	3009 ± 581.3	9.7 ± 1.9	0.02	−6.00	−5.74	−11.79
S-Citalopram	4367 ± 293.0	5.6 ± 1.0	0.01	−8.68	−3.30	−12.05
Duloxetine	2446 ± 616.8	13.1 ± 2.1	0.03	−4.86	−7.75	−12.65
Fluoxetine	2746 ± 421.8	10.4 ± 1.4	0.02	−5.46	−6.16	−11.76
Fluvoxamine	38.45 ± 439.0	18.5 ± 1.5	0.04	−0.08	−10.92	−11.04
Indatraline	1580 ± 445.4	15.0 ± 1.5	0.03	−3.14	−8.86	−12.00
Paroxetine	2765 ± 578.2	11.9 ± 2.0	0.02	−5.49	−7.03	−12.51
Sertraline	1902 ± 755.4	14.3 ± 2.6	0.03	−3.78	−8.42	−12.01
Venlafaxine	2552 ± 341.9	9.2 ± 1.2	0.02	−5.07	−5.40	−10.58

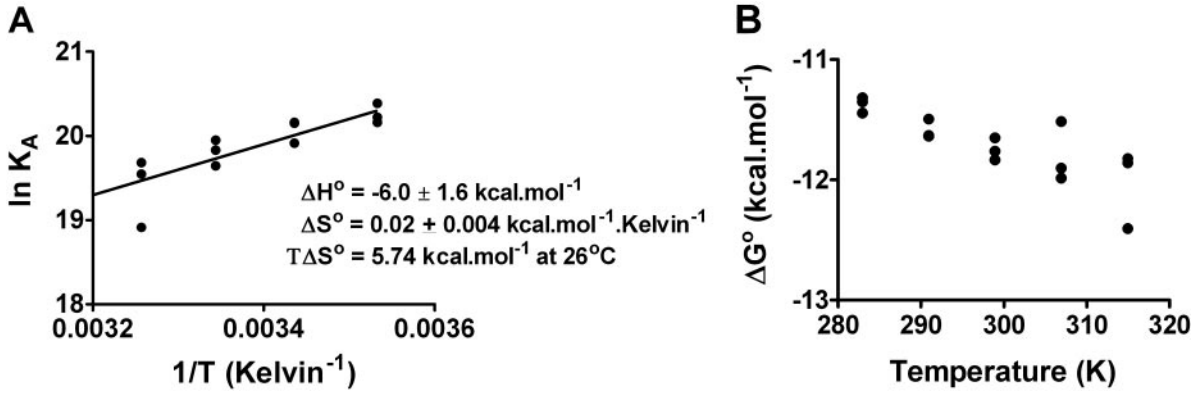

Fig. 3. Changes in equilibrium binding properties of [^{3}H]*S*-citalopram with temperature. A, van't Hoff plot of [^{3}H]*S*-citalopram affinities at hSERT determined using hSERT-HEK membranes under equilibrium conditions at controlled temperatures (10, 18, 26, 36, and 42°C). Each point plotted represents the association constant, K_A (i.e., $1/K_D$ or $1/K_I$) determined by saturation binding over 12 different radioligand concentrations each determined in triplicate. Each experiment was conducted on three independent occasions. Estimates of enthalpy (ΔH^O) and entropy (ΔS^O) associated with binding or [^{3}H]*S*-citalopram to SERT were made using the slope and y-intercept, respectively, as described in the van't Hoff equation, $\ln(K_A) = -(\Delta H^O/R) \times (1/T) + (\Delta S^O/R)$. B, calculated change in Gibbs free energy with temperature from $\Delta G^O = -RT(\ln K_A)$. This change in reaction energy is likely to reflect the temperature dependence of ΔH^O. Under the assumption that ΔS^O is constant relative to temperature, ΔH^O can be determined for every temperature from $\Delta H^O = -RT\ln(K_A) + \Delta S^O$. The observed linear change in the ΔH with temperature allowed determination of heat capacity, $C_p = [d(\Delta H^O)/T]$, from the slope.

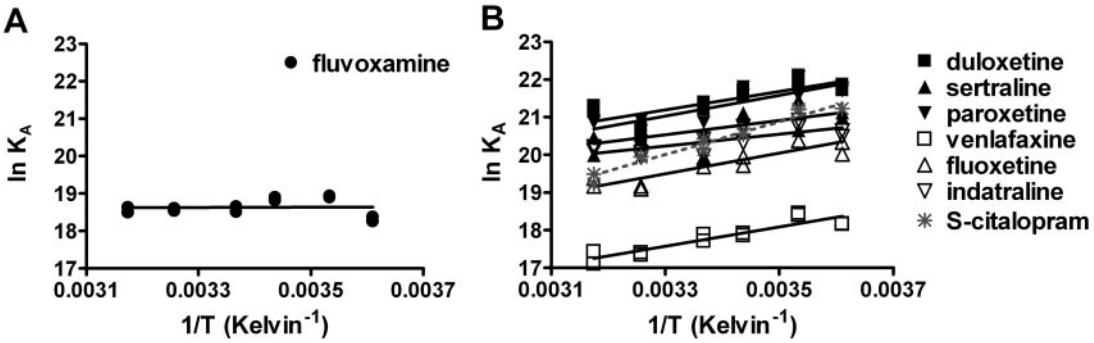

Fig. 4. van't Hoff plots for antidepressant affinities at SERT over a 4–42°C temperature range. Drug affinities are determined from displacement binding studies with [^{3}H]*S*-citalopram under equilibrium conditions (5–24-h incubation). Each point plotted represents the K_A (i.e., $1/K_I$) determined by over 12 different radioligand concentrations each determined in triplicate. Each experiment was conducted on two independent occasions. Estimates of enthalpy (ΔH^O) and entropy (ΔS^O) associated with binding of [^{3}H]*S*-citalopram to SERT were made as described for Fig. 3. Thermodynamic properties of the drugs are binned into broad categories in which enthalpy is more than -0.1 kcal · mol^{-1} (A) and -3 to -9 kcal · mol^{-1} (B). As for Fig. 3, observed linear increases in log equilibrium association affinities ($\ln K_A$) with the inverse of temperature are likely to reflect the temperature dependence of ΔH. If so, the heat capacities can be calculated from the slope of the linear relation observed between ΔH and temperature.

toward slower dissociation rate constants with increasing affinity (Fig. 7A). The kinetic constants of association for these ligands were calculated from the ratio between the kinetic constants of dissociation and the equilibrium dissociation affinity (i.e., $k_{+1} = k_{-1} \cdot K_A$; Table 1). These association rate constants showed a direct linear correlation with the equilibrium affinity constants of association for all ligands ($P = 0.0006$; Fig. 7B).

As expected, association and dissociation rates for [^{3}H]*S*-citalopram binding increased with temperature over the range tested (Fig. 8). Analysis of the observed association rate constants for [^{3}H]*S*-citalopram versus temperature revealed a linear relationship between $\log(k_{+1})$ and 1/T (Fig. 9). The Arrhenius energy of activation (E_a) inferred from the slope of this plot was 19.5 kcal · mol^{-1}.

Correlation of Ligand Physicochemical Properties and Thermodynamics of Binding to SERT. For each molecule, the polar surface area (PSA), number of hydrogen bond donors, and number of oxygen or nitrogen donors were calculated using ISIS/Draw (MDL Information Systems, Inc., San Ramon, CA). In addition, the water/*n*-octanol partition coefficients for both neutral and ionized solutes (log P and log $D^{7.4}$, respectively) were measured, along with the acid ionization constant (pK_a). All values are summarized in Table 3. The PSA values for all molecules were low, consistent with their ability to diffuse across lipid membranes and enter the brain to evoke their antidepressant or psychostimulant effects. There was no correlation between PSA and ΔG^O, reaction rate constants, or equilibrium dissociation constant. However, for all molecules except fluvoxamine a correlation between PSA and observed changes in both enthalpy and entropy was observed ($P = 0.04$ and 0.06, respectively; Fig. 10). Significant correlation was also observed with the numbers of rotatable bonds and enthalpy or entropy ($P = 0.04$ and 0.05, respectively; Fig. 11B). The measured partition coefficients fell into a relatively narrow range (log P = 3–4.1, log $D^{7.4}$ = 0.8–2.3, respectively). All compounds were monobases, with pK_a values of 8.1 to 9.7 and are consequently

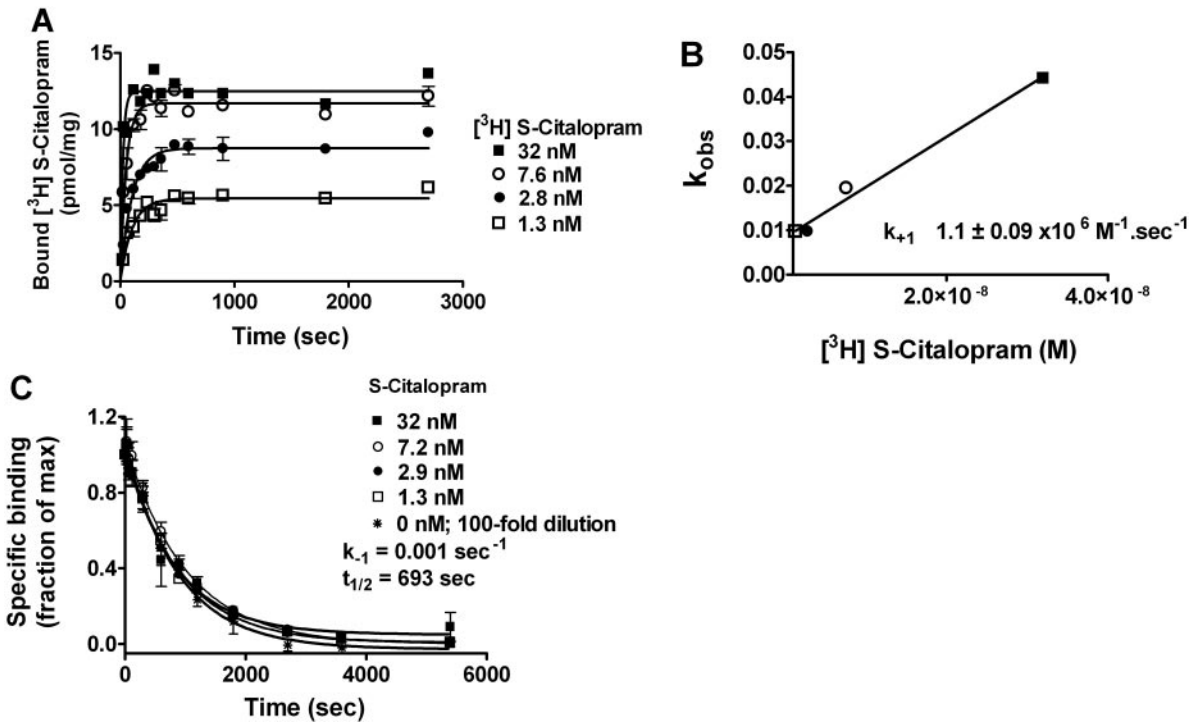

Fig. 5. Association and dissociation binding of [^{3}H]*S*-citalopram. A, time course of association of [^{3}H]*S*-citalopram to hSERT-HEK membranes, including nonlinear regression to exponential growth equation, describing the amount of specifically bound [^{3}H]*S*-citalopram = $\max \cdot 1 - e^{-k_{obs}[\cdot t]}$), where k_{obs} is the observed rate constant that is dependent on administered radioligand concentration, [L*]. B, plot of k_{obs} versus radioligand concentration for the data presented in A to determine concentration-independent association rate constant, k_{+1}, from observed associations rates using the relation $k_{obs} = k_{+1}$.[radioligand] + k_{-1}. C, time course of dissociation of [^{3}H]*S*-citalopram from hSERT-HEK membranes following addition of varying concentrations of unlabeled *S*-citalopram or 100-fold dilution of radioligand in assay buffer.

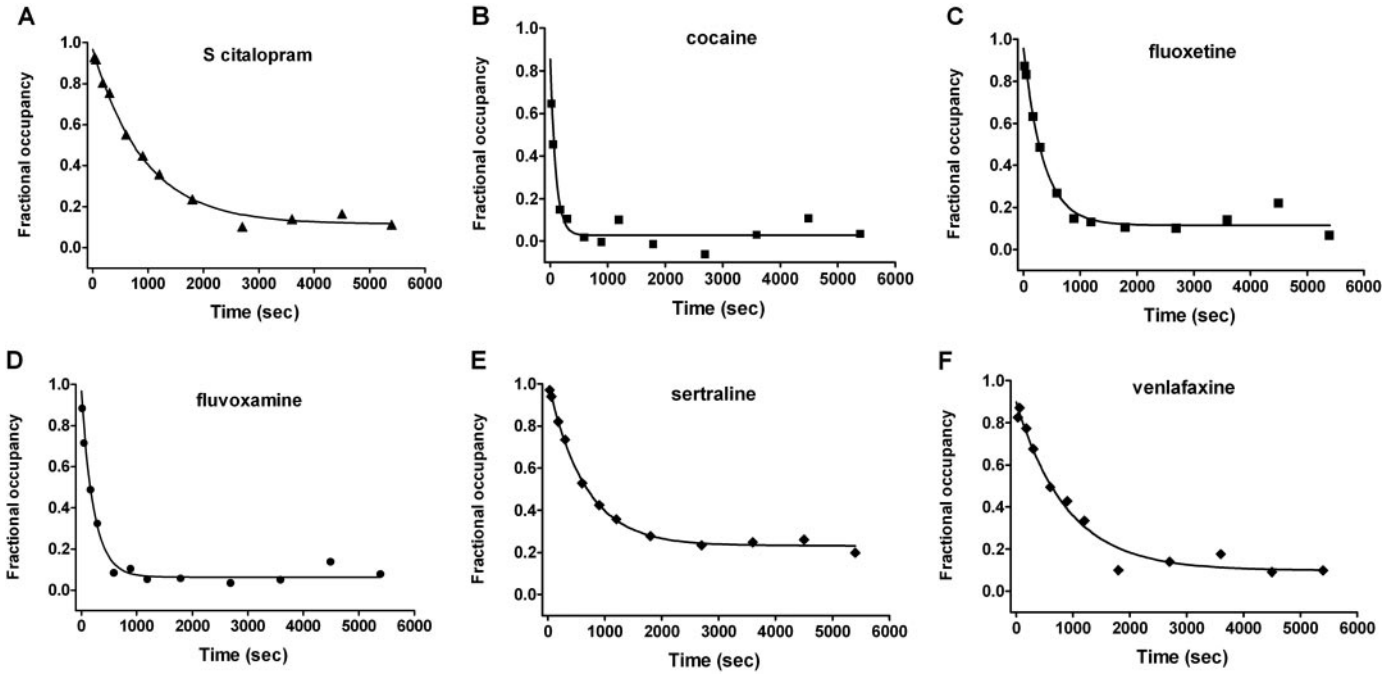

Fig. 6. Dissociation kinetics of *S*-citalopram (A), cocaine (B), fluoxetine (C), fluvoxamine (D), sertraline (E), and venlafaxine (F) determined using the competitive dissociation method with [^{3}H]*S*-citalopram. Data show the time course of dissociation of unlabeled ligand from hSERT-HEK membranes as inferred from the rate of association of [^{3}H]*S*-citalopram (40–60 nM). Each graph show representative data from a single experiment in which specifically bound radioligand, [R · L*] was determined in the absence or presence of competing ligand at multiple time points, *t*, was determined in triplicate. Fractional occupancy is calculated from fractional occupancy = $\{1 - ([R \cdot L^*]_t^{\text{with competitor}})/([R \cdot L^*]_\infty^{\text{no competitor}})\}$. In this context, $t = \infty$ represents the equilibrium condition at which bound radioactivity is less than 20% of the preceding time point for at least three sequential time points. In all cases, changes in fractional occupancy with time were fitted to a simple exponential decay equation ($y = Ae^{-kt} + c$, where $-k$ is the dissociation rate constant, and A and c are constants) and goodness of fit, R^2, was >0.9. Mean dissociation rate constants and half-lives for these and other ligands, determined in two to six independent experiments, are summarized in Table 1.

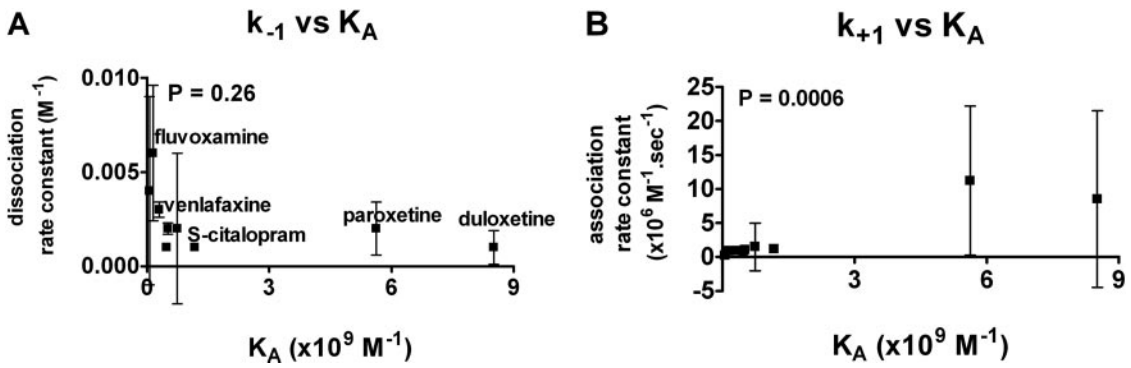

Fig. 7. Graphical representation of rate constants for dissociation (k_{-1}) (A) and association (k_{+1}) (B) versus equilibrium association constants [$K_A = (1/K_D) = (k_{+1}/k_{-1})$] for SERT inhibitors. Plotted k_{-1} values show the observed mean and standard deviation of the dissociation rate constant for a given drug determined from two to four separate experiments determined at room temperature. Plotted k_{+1} values are calculated for each drug from measured values of K_D and k_{-1} using the following relationship: $k_{+1} = (k_{-1}/K_D) = (k_{-1} \times K_A)$. In general, the higher affinity ligands have both slower dissociation and slower association rates (for a given –fold concentration relative to its affinity). A significant correlation between k_{+1} (but not k_{-1}) and K_A was observed by two-tailed Pearson correlation ($P = 0.0006$).

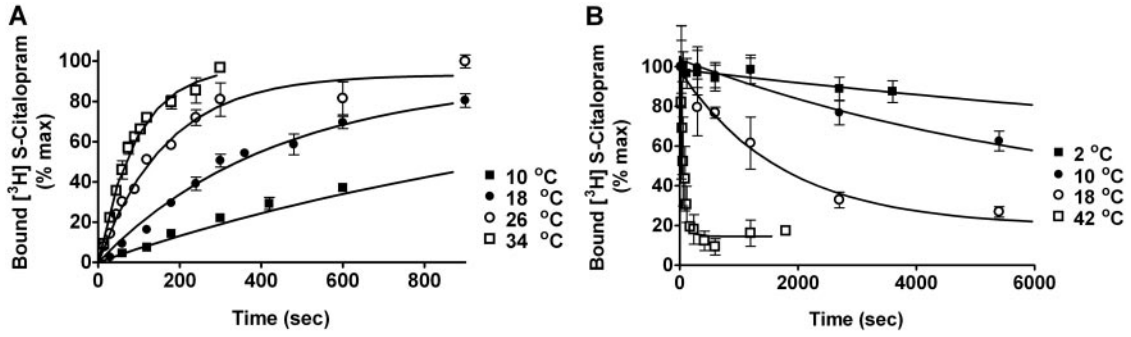

Fig. 8. Effects of temperature on association (A) and dissociation (B) kinetics of [^{3}H]*S*-citalopram binding to hSERT-HEK membranes. Data are presented from representative experiments, in which binding kinetics of [^{3}H]*S*-citalopram (2.5 nM for association; 8–10 nM for dissociation) were determined under controlled temperatures (2, 10, 18, 26, 36, or 42°C). Each data point is the mean and standard deviation of three replicate determinations.

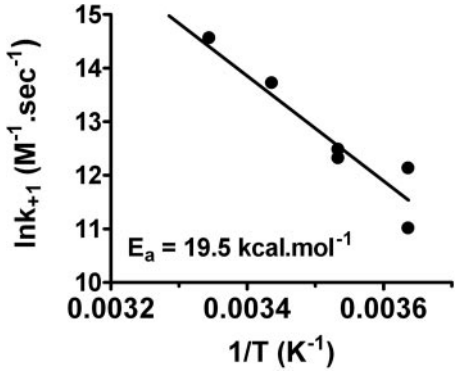

Fig. 9. Arrhenius plot showing the effect of temperature on the association rate constants of [^{3}H]*S*-citalopram determined at 2, 10, 18, 24, and 36°C. The E_a value for the ligand-receptor binding is determined from slope of the best-fit line described by the Arrhenius equation, $\ln k_{+1} = \ln A - [(E_a/R) \times (1/T)]$. Each data point plotted represents a single estimate of k_{+1} determined from global analysis of within-day observations of k_{obs} at a given temperature using at least four different concentrations of radioligand (1–33 nM). Methods and analysis are similar to those described for Fig. 5, with the introduction of the controlled variable of temperature.

predicted to be predominantly in the protonated form at physiological pH. Unlike with PSA, there was no relationship between measured partition coefficients and reaction thermodynamic parameters.

Discussion

SERT inhibition is a proven treatment for depression and anxiety disorders. However the current absence of high-resolution molecular models for SERT precludes rigorous structure-based design of molecules that block its serotonin reuptake activity. Specifically lacking are models that explicitly compute the nature and relative contributions of interactions occurring between the inhibitor and transporter, assess the ligand surface area buried by that interaction, and account for SERT conformational transitions stabilized by the ligand. A homology model for the interaction of SERT with inhibitors was recently proposed, based on bacterial leucine transporter (Ravna et al., 2006a). More recently, cocrystallization of antidepressant with the homologous LeuT was reported (Singh et al., 2007; Zhou et al., 2007). However, there are two serious limitations with the use of these models. First, although most SERT inhibitors seem to be competitive with 5-HT (Apparsundaram et al., 2008), these ligands have been found to interact with LeuT at extremely low affinities (millimolar or worse) at a binding site that is structurally distinct from the leucine binding site. Second, structure-function and pharmacological analyses with several competitive SERT inhibitors and multiple site-directed SERT variants indicate that the LeuT-based model may not recapitulate key features of SERT ligand binding and trans-

TABLE 3

Chemical properties of SERT inhibitors

Values for PSA, the number of oxygen or nitrogen donors (num_ON), and the number of hydrogen donors (num_H) were calculated by ISIS/Draw software. Values for partition coefficients log P and log $D^{7.4}$ and acid ionization constant (pK_a) were measured using the potentiometric titration method. The numbers of rotatable bonds were computed using MOE software from the Chemical Computing Group (Montreal, QC, Canada). The conformers were computed using the OMEGA software.

	PSA	Num_ON	Num_H	Log P	Log $D^{7.4}$	pK_a	No. of Rotatable Bonds	No. of Allowed Conformations
S-Citalopram	34.37	3	0	3.63	1.49	9.54	6	7
Cocaine	44.06	5	0				5	10
Duloxetine	19.39	2	1	3.76	1.6	9.56	6	40
Fluoxetine	19.66	2	1	3.9	1.57	9.72	7	21
Fluvoxamine	48.25	4	2	4.08	2.21	9.27	10	114
Indatraline	11.99	1	1	3.38	2.17	8.58	2	6
Paroxetine	39.63	4	1	3.55	1.29	9.66	4	31
Sertraline	11.48	1	1	3.07	2.26	8.13	2	4
Venlafaxine	26.97	3	1	3	0.78	9.62	5	7

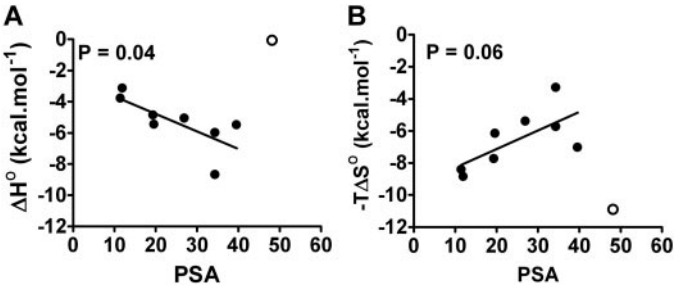

Fig. 10. Relationship between PSA and enthalpy (A) and entropy ($-T\Delta S^O$) (B). In all cases, the fluvoxamine data are presented as an open symbol and excluded from linear regression analyses. Values for enthalpy and entropy at 24–26°C were determined for all ligands by van't Hoff analysis of the change in equilibrium binding affinity with temperature (as presented in Table 2 and Fig. 4). Outcomes of correlation analyses using two-tailed Pearson correlation are presented as *P* values.

port reactions, including sensitivity to potassium, lack of chloride dependence in leucine transport, and very low 20% sequence homology between transport proteins (Yamashita et al., 2005; Zhang and Rudnick, 2005; Rudnick, 2006). In the absence of robust models to guide structure-activity relationships, it is of great importance to dissect and understand the thermodynamic parameters driving inhibitor binding. We have undertaken this task using a well characterized set of SERT competitive inhibitors (Apparsundaram et al., 2008).

This study makes deliberate use of the stereospecific radioligand [^{3}H]*S*-citalopram to avoid confounds of mixed ligand affinities of the *S*- and *R*-enantiomers present in racemic SERT ligands, including citalopram. Our observed equilibrium dissociation constants are similar to those reported previously for these SERT inhibitors (Tatsumi et al., 1997; Nemeroff and Owens, 2003). More importantly, we report here for the first time on the kinetics of binding of several SERT inhibitors. We found that the first order dissociation rate constant varies only 6-fold for the compound set that we used (Table 1). Therefore, observed equilibrium binding constants seem to be more influenced by the rate constants for association than dissociation. Theoretically, the methods used here for determination of dissociation rate constants suffer from two key theoretical limitations: 1) the inferred rate of test ligand dissociation is not confounded by the rate of radioligand association, and 2) radioligand binding must bind in a mutually exclusive manner with all the test ligands. However, empirical data to address both of these concerns is provided. First, the directly measured dissociation rate constants for both [^{3}H]*S*-citalopram and [^{3}H]paroxetine, determined by dilution-evoked dissociation, are in good agreement with those determined for their unlabeled homologs, *S*-citalopram and paroxetine, by the competitive dissociation method. Second, in the companion study, Apparsundaram et al. (2008) carefully demonstrate that in all cases, text ligands bind in a manner that is competitive (i.e., mutually exclusive) with [^{3}H]*S*-citalopram.

From measured equilibrium binding affinities at different temperatures, the relative contributions of entropic and enthalpic changes to reaction energetics, determined from van't Hoff analyses, were determined to be roughly similar (25–75% of the total binding energy) across all ligands, with the exception of fluvoxamine, which was entropy-predominant. Even drugs that lie at the extremes of the range in terms of association rate constants (paroxetine and venlafaxine) were found to have similar relative contributions of enthalpy or entropy to the Gibbs free energy change, suggesting that slow association does not seem to be driven by significant increase in, e.g., conformational change. The gains in enthalpy with increasing polar surface area suggest that the inhibitor binding pocket allows for formation of electrostatic or polar interactions without significant desolvation penalty.

In all cases, the relationship between $\ln K_A$ and 1/T was linear, presumably reflecting a linear relationship between temperature and enthalpy, resulting from a constant C_p across the experimental temperature range. This implies a lack of substantial conformational change upon binding that would incur desolvation of hydrophobic surfaces (Todd et al., 1998). However, direct measurement of the influence of temperature on the forward kinetic constant of [^{3}H]*S*-citalopram binding yielded an E_a estimate of 19.5 kcal $\cdot$ mol^{-1} for this reaction. This value is higher than would be expected for a diffusion-controlled reaction (5–8 kcal $\cdot$ mol^{-1}), and more typical of reactions in which the heat capacity changes with temperature: CaMKII autophosphorylation (18 kcal $\cdot$ mol^{-1}) (Bradshaw et al., 2002), T4 lysozyme and Arc repressor folding (19 and 15 kcal $\cdot$ mol^{-1}, respectively) (Chen et al., 1989; Milla and Sauer, 1994).

Although apparently incongruous, the observations of high E_a and temperature-independence of C_p can coexist if compensatory, small, self-cancelling effects contribute to ΔC_p. This seems a likely scenario given the relatively small area that the ligand binding site encompasses by comparison with the size of the extracellular face of the transporter. Furthermore, the contributions of polar and nonpolar interactions between ligand and transporter are likely to oppose each other's impact on ΔC_p.

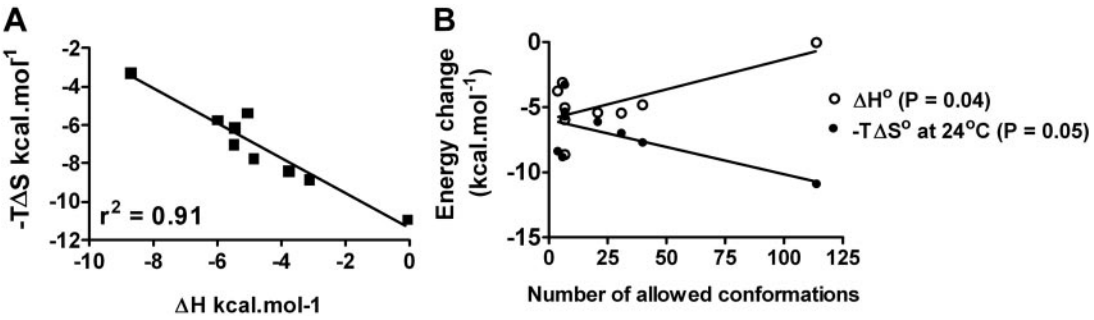

Fig. 11. A, inverse correlation between entropy ($-T\Delta S^O$) and enthalpy (ΔH^O) for all ligands in this series (including fluvoxamine) demonstrating entropy-enthalpy compensation. B, relationships between entropy ($-T\Delta S^O$; solid symbols) or enthalpy (ΔH^O; open symbols) and the calculated number of allowed conformations for each ligand tested. Values for enthalpy and entropy at 24–26°C were determined for all ligands by van't Hoff analysis of the change in equilibrium binding affinity with temperature (as presented in Table 2 and Fig. 4). Outcomes of correlation analyses using two-tailed Pearson correlation are presented as *P* values.

Compared with other membrane-bound receptors, small-molecule agonist and antagonist interactions at G protein-coupled receptors and ion channels at similar ΔG values (5–10 kcal · mol^{-1}), bind in both enthalpy- and entropy-predominant components (Borea et al., 2000), indicating minimal contribution of postulated agonist-induced conformational changes to binding energetics. In that analysis, linear van't Hoff plots predict similar temperature independence of heat capacities, possibly attesting to a comparatively small impact of ligand on overall protein structure.

An examination of the observed binding energetics with the physicochemical properties of the SERT inhibitors revealed that enthalpy increased with polar surface area across all ligands, except fluvoxamine. These data suggest a SERT inhibitor binding site that is polar and that allows presumably (protonated) hydrated ligands to bind without imposing the enthalpic penalty expected from ligand dehydration (approximately 2.5 kcal · mol^{-1} for every bond). · This might hypothetically place the binding site along the aqueous pore traversed by 5-HT, Na^+, and Cl^- (Rudnick, 2006). Consistent with this, various studies using engineered mutations, to define the transport path and the residues that underlie high-affinity binding of inhibitors, place the inhibitor binding site in the SERT transporter within the aqueous permeation path traversed by 5-HT, Na^+, and Cl^-. Furthermore, very recent data (Apparsundaram et al., 2008) demonstrate for the first time that 5-HT and the SERT inhibitors bind in a mutually exclusive, competitive manner in the wild-type serotonin transporter in spite of the different amino acid residues that subserve these interactions.

The exceptional entropic behavior observed with fluvoxamine suggests that the inhibitor binding pocket on this transport protein must allow for more than one mode of interaction. Of all the ligands tested in this study, fluvoxamine possesses the highest rotational freedom, with 114 potential conformations accessible. Potent, entropy-predominant binding of such a ligand suggests the potential for a second binding mode in this receptor that is fueled by energy release upon burying hydrophobic ligand moieties into the binding pocket while being flexible enough to suffer minimal loss in entropy from conformational constraint. Recent data place the two binding modes close to each other and at or near the aqueous 5-HT transit pore because 5-HT, fluvoxamine, and several of the more enthalpic ligands (*S*-citalopram, paroxetine, and venlafaxine) were found to bind competitively with radiolabeled SERT inhibitors (Apparsundaram et al., 2008). Although we can conclude from these pharmacological data that the ligands bind in a mutually exclusive manner, we cannot deduce whether these binding sites are truly colocalized. The molecular determinants of the fluvoxamine binding pocket remain to be elucidated by receptor mutagenesis studies or ligand-transporter cocrystallography.

The inverse correlation between entropy and enthalpy changes across all of the inhibitors in this study, including fluvoxamine, is consistent with the more general phenomenon of entropy-enthalpy compensation in ligand-protein interactions in which gains in enthalpy from strengthening ligand-receptor bonds (e.g., van der Waals interactions) are counteracted by concomitant losses in entropy due to a combination of conformational and solvation effects (Velazquez-Campoy et al., 2000; Ruben et al., 2006; Lafont et al., 2007). Thus, the relative contributions of entropy and enthalpy across this series of drugs follows a spectrum of allowed behaviors from ligand binding to proteins with larger conformational flexibility or hydrophobic properties (allowing larger entropy) to ligands inducing H-bond and van der Waals interactions with little energetic cost due to H-bond disruption upon dehydration (allowing larger enthalpy). The allowance for different interactions (as manifested by the two proposed binding modes that are exemplified by citalopram and fluvoxamine) suggests that the SERT binding pocket will tolerate diversity in the types of interactions that render high affinity. This increases the theoretically exploitable space for new, high-affinity SERT inhibitors. The harder question, which this study on its own cannot address, is whether all of this exploitable space is equally useful in the context of antidepressant clinical efficacy.

Acknowledgments

We are indebted to Robert Weikert (Department of Medicinal Chemistry, Roche Pharmaceuticals, Palo Alto, CA) and Mohammad Masjedizadeh (Department of Radiochemistry, Roche Pharmaceuticals) for synthesis of labeled and unlabeled *S*-citalopram. Finally, we thank Michael Bradshaw, James C. Lee, Robert T. Sauer, and Ernesto Freire for advice and discussions.

References

Apparsundaram S, Stockdale DJ, Henningsen RA, Milla ME, and Martin RS (2008) Antidepressants targeting the serotonin reuptake transporter act via a competitive mechanism. *J Pharmacol Exp Ther* **327:**982–990.

Blakely RD, Berson HE, Fremeau RT Jr, Caron MG, Peek MM, Prince HK, and Bradley CC (1991) Cloning and expression of a functional serotonin transporter from rat brain. *Nature* **354:**66–70.

Blakely RD, De Felice LJ, and Hartzell HC (1994) Molecular physiology of norepinephrine and serotonin transporters. *J Exp Biol* **196:**263–281.

Bonnet JJ, Benmansour S, Costentin J, Parker EM, and Cubeddu LX (1990) Thermodynamic analyses of the binding of substrates and uptake inhibitors on the neuronal carrier of dopamine labeled with [^{3}H]GBR 12783 or [^{3}H]mazindol. *J Pharmacol Exp Ther* **253:**1206–1214.

Borea PA, Dalpiaz A, Varani K, Gilli P, and Gilli G (2000) Can thermodynamic measurements of receptor binding yield information on drug affinity and efficacy? *Biochem Pharmacol* **60:**1549–1556.

Boström J, Greenwood JR, and Gottfries J (2003) Assessing the performance of OMEGA with respect to retrieving bioactive conformations. *J Mol Graph Model* **21:**449–462.

Bradshaw JM, Hudmon A, and Schulman H (2002) Chemical quenched flow kinetic studies indicate an intraholoenzyme autophosphorylation mechanism for Ca^{2+}/calmodulin-dependent protein kinase II. *J Biol Chem* **277:**20991–20998.

Chen BL, Baase WA, and Schellman JA (1989) Low-temperature unfolding of a mutant of phage T4 lysozyme. 2. Kinetic investigations. *Biochemistry* **28:**691–699.

Chen F, Larsen MB, Neubauer HA, Sánchez C, Plenge P, and Wiborg O (2005a) Characterization of an allosteric citalopram-binding site at the serotonin transporter. *J Neurochem* **92:**21–28.

Chen F, Larsen MB, Sánchez C, and Wiborg O (2005b) The *S*-enantiomer of *R,S*-citalopram, increases inhibitor binding to the human serotonin transporter by an allosteric mechanism. Comparison with other serotonin transporter inhibitors. *Eur Neuropsychopharmacol* **15:**193–198.

Cheng Y and Prusoff WH (1973) Relationship between the inhibition constant (K1) and the concentration of inhibitor which causes 50 per cent inhibition (I50) of an enzymatic reaction. *Biochem Pharmacol* **22:**3099–3108.

Claassen V, Davies JE, Hertting G, and Placheta P (1977) Fluvoxamine, a specific 5-hydroxytryptamine uptake inhibitor. *Br J Pharmacol* **60:**505–516.

Henry LK, Field JR, Adkins EM, Parnas ML, Vaughan RA, Zou MF, Newman AH, and Blakely RD (2006) Tyr-95 and Ile-172 in transmembrane segments 1 and 3 of human serotonin transporters interact to establish high affinity recognition of antidepressants. *J Biol Chem* **281:**2012–2023.

Lafont V, Armstrong AA, Ohtaka H, Kiso Y, Mario Amzel L, and Freire E (2007) Compensating enthalpic and entropic changes hinder binding affinity optimization. *Chem Biol Drug Des* **69:**413–422.

Milla ME and Sauer RT (1994) P22 Arc repressor: folding kinetics of a single-domain, dimeric protein. *Biochemistry* **33:**1125–1133.

Nemeroff CB and Owens MJ (2003) Neuropharmacology of paroxetine. *Psychopharmacol Bull* **37 (Suppl 1):**8–18.

Partilla JS, Dersch CM, Yu H, Rice KC, and Rothman RB (2000) Neurochemical neutralization of amphetamine-type stimulants in rat brain by the indatraline analog (−)-HY038. *Brain Res Bull* **53:**821–826.

Perola E and Charifson PS (2004) Conformational analysis of drug-like molecules bound to proteins: an extensive study of ligand reorganization upon binding. *J Med Chem* **47:**2499–2510.

Ravna AW, Jaronczyk M, and Sylte I (2006a) A homology model of SERT based on the LeuT(Aa) template. *Bioorg Med Chem Lett* **16:**5594–5597.

Ravna AW, Sylte I, Kristiansen K, and Dahl SG (2006b) Putative drug binding conformations of monoamine transporters. *Bioorg Med Chem* **14:**666–675.

Rothman RB and Baumann MH (2003) Monoamine transporters and psychostimulant drugs. *Eur J Pharmacol* **479:**23–40.

Ruben AJ, Kiso Y, and Freire E (2006) Overcoming roadblocks in lead optimization: a thermodynamic perspective. *Chem Biol Drug Des* **67:**2–4.

Rudnick G (2006) Serotonin transporters–structure and function. *J Membr Biol* **213:**101–110.

Singh SK, Yamashita A, and Gouaux E (2007) Antidepressant binding site in a bacterial homologue of neurotransmitter transporters. *Nature* **448:**952–956.

Tatsumi M, Groshan K, Blakely RD, and Richelson E (1997) Pharmacological profile of antidepressants and related compounds at human monoamine transporters. *Eur J Pharmacol* **340:**249–258.

Todd MJ, Semo N, and Freire E (1998) The structural stability of the HIV-1 protease. *J Mol Biol* **283:**475–488.

Velazquez-Campoy A, Todd MJ, and Freire E (2000) HIV-1 protease inhibitors: enthalpic versus entropic optimization of the binding affinity. *Biochemistry* **39:**2201–2207.

White KJ, Walline CC, and Barker EL (2005) Serotonin transporters: implications for antidepressant drug development. *AAPS J* **7:**E421–E433.

Wong DT, Bymaster FP, Mayle DA, Reid LR, Krushinski JH, and Robertson DW (1993) LY248686, a new inhibitor of serotonin and norepinephrine uptake. *Neuropsychopharmacology* **8:**23–33.

Yamashita A, Singh SK, Kawate T, Jin Y, and Gouaux E (2005) Crystal structure of a bacterial homologue of Na+/Cl–dependent neurotransmitter transporters. *Nature* **437:**215–223.

Zhang YW and Rudnick G (2005) Cysteine-scanning mutagenesis of serotonin transporter intracellular loop 2 suggests an α-helical conformation. *J Biol Chem* **280:**30807–30813.

Zhou Z, Zhen J, Karpowich NK, Goetz RM, Law CJ, Reith ME, and Wang DN (2007) LeuT-desipramine structure reveals how antidepressants block neurotransmitter reuptake. *Science* **317:**1390–1393.

Address correspondence to: Dr. Renee Martin, Roche Pharmaceuticals, 3431 Hillview Ave., Palo Alto CA 94304. E-mail: renee.martin@roche.com